ORTHOGONAL PLANE OF WEAKNESS MODEL FOR MASONRY ASSEMBLAGES

Kwesi A. Andam, PhD CEng FICE FGhIE
Department of Civil Engineering, U. S. T., Kumasi, Ghana.

ABSTRACT

Brick masonry assemblage composed of brick mass, head joint, and bed joint is subjected to uniaxial compressive stress regime. The compressive stress is increased until failure occurs as the bed joint is rotated through O - π/2.

The results of this test compare favourably with previous finite element simulation. The orthogonal plane of weakness theory, a modified version of a similar phenomenon found in rock mechanics is now applied to masonry assemblages.

Keywords:*masonry, orthogonal plane of weakness, uniaxial stress, struve functions.*

Nomenclature

f_c	compression stress at failure
f_t	tensile stress at failure
f_{tb}, f_{cb}	uniaxial strength of brick
f_m	axial compression in masonry
f_b, f_b	uniaxial compression strength of brick
f_{bt}	strength of brick under biaxial tension
f_j, f_j	uniaxial compressive strength of mortar
f_c	compressive stress at failure
U_u	non-uniformity coefficient at failure
F_m	yield function
T_c	critical shear stress
σ_n	normal stress
σ_{ult}	ultimate yield stress of a prism
ε	strain vector
	vector increment
	compliance matrix
E_i	Young's modulus
G_i	shear modulus
v	Poisson ratio
J_i	Bessel function
H_i	Struve function
ε^{ve}	viscoelastic component
a	bed joint orientation

INTRODUCTION

Masonry assemblages as two-phase composites comprising brick and mortar are fashioned along well known traditional bonds such as Flemish and Quetta. A common feature of each bond [Figure 1] is that the assemblage is inherently composed of a *continuous* horizontal mortar joint (bed joint) and a *discontinuous* vertical mortar joint (head joint). The constituents of an unreinforced masonry matrix are therefore:

i. brick mass

ii. bed joint (mortar)

iii. head joint (mortar)

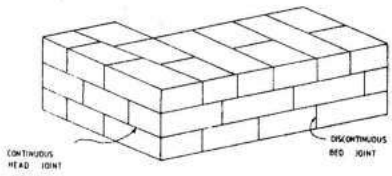

Fig. 1: Orthogonal Joint Set

Kwesi A. Andam

In this test, the mortar/brick interface was highly sensitive and necessitated the use of diamond saws to pre-shape angular edges of bricks prior to the assembling of the masonry matrix. Prisms were cured by simply covering them with soaked sacks over the 28-day period. Figure 2 shows the test rig.

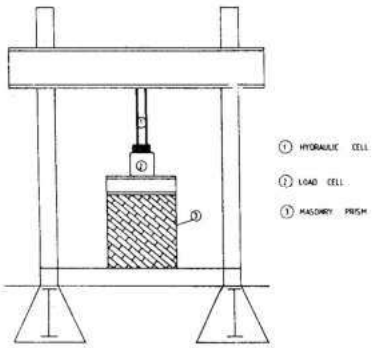

Fig. 2: Uniaxial Compression Test Rig

Mechanisms of failure

The development of cracks within the prism at the intermediate and ultimate stages, during the test, was chronologically recorded.

$$\alpha = 0$$

The first network of sparsely distributed hairline cracks running perpendicular to head joints appeared when in-plane stress was about $0.7\sigma_{ult}$. These cracks were confined to within the brick mass and head joints and grew in quality until ultimate failure was reached (Figure 3a).

$$\sigma = 0.04\pi$$

The cracks delayed considerably in forming and appeared around $0.88\sigma_{ult}$ when hairline cracks parallel to the bed joint and confined to the middle section of the prism first appeared. The ultimate failure was generally explosive (Figure 3b).

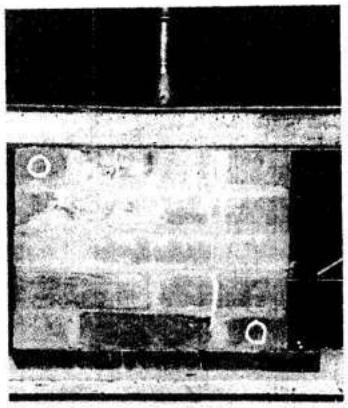

Fig. 3(a) : Crack Mechanism - Primary Tensile Strength

$$\alpha = 0.08\pi$$

The first cracks started developing around $0.69\sigma_{ult}$ running parallel to the head joints. These cracks were confined to within the brick mass and head joints and grew in quantity until ultimate failure was reached.

$$\alpha = 0.12\pi$$

Fig. 3(b) : Crack Mechanism - Transition Zone

Around $0.45\sigma_{ult}$ there was evidence of the bed joints separating in shear and at the same time short cracks forming in the bricks mass parallel to the head joints. The ultimate loads were among the least in all the tests.

$$\alpha = 0.19\pi$$

The first cracks developed quite early around $0.44\sigma_{ult}$ in the head joints and brick mass and parallel to the head joint (Figure 3c). The initial cracks grew in number in a similar manner until ultimate load was reached.

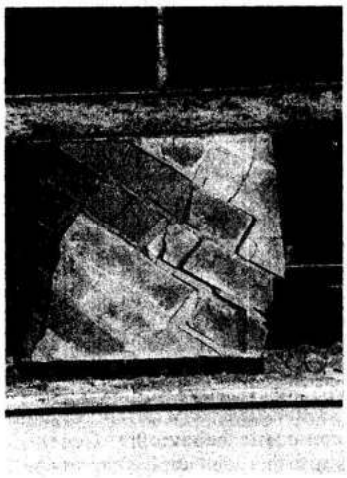

Fig. 3c: Crack Mechanisms - Combined Shear and Tensile Strength

$$\alpha = 0.25\pi$$

The first cracks delayed considerably and formed around $0.86\sigma_{ult}$ mainly in the brick mass. The failure loads were relatively high and second to those encountered in the $\alpha = 0$ test.

$$\alpha = 0.31\pi$$

The head joint now began to separate in shear. Though there were cracks in the mass as well, the pattern of cracks changed from the previous test. First cracks appeared at $0.56\sigma_{ult}$ heralding a transition from shear in bed joints to shear in head joints.

$$\alpha = 0.37\pi$$

Relative to the previous tests, the failure load decreased though the mechanism of failure remained the same. First cracks appeared around $0.32\sigma_{ult}$.

$$\alpha = 0.42\pi$$

The first cracks delayed and appeared around $0.8\sigma_{ult}$. The same pattern of failure as $\alpha = 0.31\pi$ and $\alpha = 0.37\pi$ was observed. While the bed joints and brick mass suffered crushing, the head joints separated in shear (Figure 4).

Fig. 4: Primary Shear Failure

$$\alpha = 0.45\pi$$

The most spectacular crushing of the brick mass in the middle section of the prism took place after the mortar in the head joints had similarly failed in tension. Failure loads were amongst the highest though lower than $\alpha = 0$, and $\alpha = 0.25\pi$.

Constitutive relations for orthogonality

The earlier work is now modified to account for the peculiar *orthogonal effect*. A rheological analogue (Figure 5) comprising springs and dashpots simulate assembly behaviour through elastic, viscous and delayed elastic responses. Constitutive relations for this four parameter model assume that any stressing of the assembly will result in corresponding two-part elasto and viscoelastic strain responses.

Thus

$$\Delta\varepsilon = \Delta\varepsilon^{e} + \Delta\varepsilon^{ve} \quad (4)$$

$$\sigma = f(\varepsilon) \quad (5)$$

The stress-strain relation is

$$\frac{\sigma}{f_b} + \frac{\sigma}{f_j} = \varepsilon \quad (6)$$

ie

$$\left\{\frac{1}{f_b}\{\delta_t\} + \frac{1}{f_j}\right\}\sigma = \{\delta_t\}\varepsilon \quad (7)$$

or

$$\sigma = \left\{\frac{1}{f_b}\{\delta_t\} + \frac{1}{f_j}\right\}\{\delta_t\}\varepsilon \quad (8)$$

for total orthogonal effect in two planes of weakness,

$$\sigma = 2f_j\varepsilon + \frac{1}{\{\delta_t\}\varepsilon} f_b\varepsilon + \frac{\varepsilon}{\left\{\frac{1}{f_b}\{\delta_t\} + \frac{2}{f_j} + \frac{1}{f_b}\right\}} \quad (9)$$

ie

$$\left\{\frac{1}{f_b}\{\delta_t\} + \frac{1}{f_j}\right\}\sigma = \left\{\frac{1}{f_b}\{\delta_t\} + \frac{2}{f_j} + \frac{1}{f_b}\right\}\left\{2f_j\varepsilon + f_b\varepsilon\right\} + \varepsilon \quad (10)$$

expanding,

$$\frac{\sigma}{f_b} + \frac{\sigma}{f_j} + \frac{\sigma}{f_b} =$$

$$\frac{2f}{f_b}\{\delta^3_t\}\varepsilon + 6\varepsilon + \frac{2f_b}{f_j}\varepsilon + \frac{2f_j}{f_b}\varepsilon + \varepsilon \quad (11)$$

ie

$$\frac{1}{f_b}\{\delta^2_t\}\sigma + \left\{\frac{1}{f_j} + \frac{1}{f_b}\right\}\{\delta_t\}\sigma =$$

$$\frac{2f_j}{f_b}\{\delta^3_t\}\varepsilon + 6\left\{1 + \frac{f_j}{3f_b}\right\}\{\delta^2_t\}\varepsilon + \left\{1 + \frac{2f_b}{f_j}\right\}\{\delta_t\}\varepsilon \quad (12)$$

In the previous work [6] in which shear-compression was also considered, it was established that:

$$\sigma_y = \sigma \sin^2\alpha \quad (13)$$

$$\sigma_x = \sigma \cos^2\alpha \quad (14)$$

$$\tau_{xy} = \sigma \cos\alpha \sin\alpha \quad (15)$$

Any one-dimensional loading will produce stresses within the assembly that must reflect on all important engineering properties of the assembly. The compliance matrices for brick mass and the orthogonal mortar zones encapsulate most of the significant engineering properties. Consider for instance, the compliance matrix for the brick mass alone:

$$[C_b] = \begin{bmatrix} \frac{1}{E_b} & \frac{v}{E_b} & 0 \\ \frac{-v_b}{E_b} & \frac{1}{E_b} & 0 \\ 0 & 0 & \frac{1}{G_b} \end{bmatrix}$$

Define ω as the assembly compliance matrix to represent composite behaviour. Generalizing all expressions up to this point implies expressing the stress as a complex variable of the form

$$\{\sigma\} = f(\alpha, \omega) \quad (18)$$

ie

$$\{\sigma\} = \sigma_o e^{i\omega \sin\sigma)} \quad (17)$$

The path of this integral through $0 - \pi/2$ is given by

$$\int_0^{\pi/2} e^{i\omega \sin\alpha} d\alpha =$$

$$\int_0^{\pi/2} [\cos(\omega \sin\alpha) + i \sin(\omega \sin\alpha)]\, d\alpha \quad (18)$$

$$= \int_0^{\pi/2} \cos(\omega \sin\alpha)\, d\alpha +$$

$$\int_0^{\pi/2} (\omega \sin\alpha - \frac{\omega^3}{3!}\sin^3\alpha + \frac{\omega^5}{5!}\sin^5\alpha - \frac{\omega^7}{7!}\sin^7\alpha + \ldots) d\alpha \quad (19)$$

Computing these high order transcendental powers will give

$$\{\sigma\} = 1/2\pi J_0(\omega)+1/2\pi H_0(\omega) \qquad (20)$$

Equation 20 is immediately recognized as a Struve function incorporating within the limits 0 - $\pi/2$ two second order curves intercepted by near-flat plains (Figure 6).

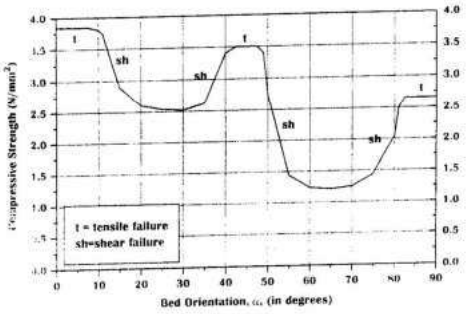

Fig. 6: Uniaxial Compression Failure Envelope

DISCUSSION

The test results should now be evaluated in relation to previous works that have been referred to in this paper.

Assemblage failure mode

Figure 6 is a unique failure phenomenon. The near-flat plains are found to be in the following regions:

i) 0 - 0.03π

ii) 0.23π - 0.26π

iii) 0.47π - 0.5π

The boundaries of the three regions are transition points when the nature of failure changes. In the first region tensile failure takes place in the brick mass and the lower bound is the transition from tensile failure in the brick mass to shear failure in the bed joint. This situation continues as the assemblage weakens in strength to a low value around $\alpha = 0.12\pi$. Beyond this point the assemblage regains strength up to the point 0.23π when a second tensile failure zone emerges.

The second tensile failure zone 0.23π0.26π is crucial as there appears to be a prism strength lower than the first tensile failure zone 0 - 0.3π. Beyond this region shear failure now takes place in the head joint. It is clear that the lowest prism strength occurs during this period around $\alpha = 0.37\pi$. The final tensile failure zone $\alpha = 0.47\pi$ - 0.5π is the region that the prism exhibits the least tensile strength. The maximum assemblage strength occurs around = 0.37π. This observation clearly has design implications.

Comparisons of experimental and FE simulation

Figure 7 shows the FE simulation [6] and the present work. In both cases the ultimate failure stresses are normalized to form a basis for comparison. A high degree of correlation is found in the two works. The FE simulation in the previous work [6] assumed very high assembly parameters. For instance the mean compressive strength of brick was taken to be 52N/mm^2 for the FE simulation as compared with 24.7N/mm^2. However, the assemblage uniaxial compressive strength is influenced by other parameters used in the simulation which when synchronized now with the test parameters are found to be very close.

Comparison with other works

The original *single plane of weakness* theory proposed by Jaeger [4] only established that failure was by shear of the anisotropic rock. This was quite opposed to the Walsh-Bruce theory which assumed that failure occurred due to tensile stresses. Maclamore and Gray then applied Jaeger's theory [5] and obtained a second order curve with flat plains at the shoulders.

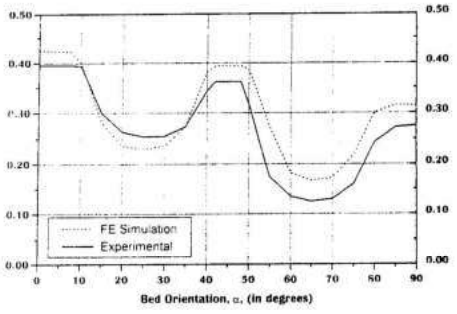

Fig. 7: Experimental and FE Simulation

In comparing the present work with those cited [4,5] it is important to bear in mind the variability of the parameters of assemblage involved. The crucial criterion is the similarity of shapes of failure envelopes obtained in the various tests. Some differences are however observed.

The *single plane of weakness* theory is only applicable to rock mechanics where failure is by shear only as proposed by Jaeger and the failure envelope is characterized by only one unique second degree curve with flat shoulders .

For masonry assemblages, failure is respectively by tensile stresses in the brick/block mass and shear in the mortar zones (Figure 6); the failure envelope is characterized by two second degree curve with three flat shoulders. It is important to distinguish the uniqueness of this failure mechanism from that of the sedimentary rocks.

CONCLUSIONS

For masonry assemblages, the concept of *orthogonal plane of weakness* is being proposed as a more appropriate modification of the *single plane of weakness* theory which is strictly applicable to sedimentary rocks.

The results of a laboratory test using masonry prisms loaded in uniaxial compression have been found to verify the applicability of orthogonal plane of weakness theory that had been previously predicted with a finite element simulation.

The behaviour of the assemblage could be accurately described with a visco-elastic model and the resultant failure envelope approximates to a Struve function.

The mechanism of failure of the assemblage is a matrix of cracking of the brick mass and separation of bed joint and head joint.

The composite strength of the assemblage, at the transition zones where the nature of failure mechanism changes, decreases with increasing bed joint orientation.

REFERENCES

1. **Hilsdorf, HK.**, *Investigation into the failure mechanism of brick masonry loaded in axial compression*, Designing, Engineering and Constructing with Masonry Products, Gulf Publishing Co., Houston, Texas, pp 33-41, 1969.

2. **Khoo, C.L. and Hendry, A.W.** *A failure criterion for brickwork in axial compression, Proceedings of the third International Brick Masonry Conference, Essen, pp 139-145, 1973.*

3. **Page, A.W.** *The biaxial compressive strength of brick masonry. Proc. Inst. Civil Engrs., Part 2, pp 893 -906, 1981*

4. **Jaeger, J.C.**, *Shear failure of anisotropic rocks*, Geol. Mag. Vol 97 No 1 pp 65-72, 1960.

5. **Mclamore, R and Gray, K.E.** *The mechanical behaviour of anisotropic sedimentary rocks.* Transactions of ASME J. Eng. Ind. Vol 89, pp 62-76, 1967.

6. **Andam, K.A.**, *Numerical evaluation of shear strength of structural assemblages*, Computer-Aided Design, Vol 19 No 7 (September 1987) pp 355-360, 1987.

7. **Graham, E.K.** *Structural properties of masonry bricks manufactured from clay deposits in Ghana*, MPhil thesis, University of Science & Technology, Kumasi, Ghana, 190p 1991.